

Supplementary Materials: Site Identity and Importance in Cosubstituted Bixbyite In_2O_3

Karl Rickert, Jeremy Harris, Nazmi Sedefoglu, Hamide Kavak, Donald E. Ellis and Kenneth R. Poeppelmeier

S1. Results

S1.1. Solid Solution Characterization

The lattice parameters of $\text{Mg}_x\text{In}_{2-2x}\text{Sn}_x\text{O}_3$, as determined from powder X-ray diffraction (XRD), and the lattice parameters of $\text{Zn}_x\text{In}_{2-2x}\text{Sn}_x\text{O}_3$, as obtained from density functional theory (DFT) computations, are provided in Figure S1. As is typical, the DFT generated lattice parameters are greater than previously reported experimental lattice parameters. Both patterns display the linear fit that is characteristic of Vegard's Law, with R^2 values of 0.9985 for $\text{Zn}_x\text{In}_{2-2x}\text{Sn}_x\text{O}_3$ and 0.9970 for $\text{Mg}_x\text{In}_{2-2x}\text{Sn}_x\text{O}_3$. The XRD patterns used for the determination of the lattice parameters of $\text{Mg}_x\text{In}_{2-2x}\text{Sn}_x\text{O}_3$ are provided in Figure S2.

S1.2. $\text{Mg}_{0.1}\text{In}_{1.8}\text{Sn}_{0.1}\text{O}_3$ Structural Refinement

Sample time-of-flight neutron and synchrotron X-ray diffraction patterns obtained from the Rietveld refinements of $\text{Mg}_{0.1}\text{In}_{1.8}\text{Sn}_{0.1}\text{O}_3$ are presented in Figure S3. These are from a refinement where Mg is present on the d-site and Sn is present on the b-site. Despite the differences in the statistical goodness-of-fit parameters that are presented in the main article, there are no obvious qualitative differences between refinements. As such, the goodness-of-fit parameters have been used to suggest the atomic occupancies. As can be observed from the inset in Figure S3, there is an asymmetric peak shape to the main peak, and this asymmetry is systematically present on every reflection. As shown by the inset, the computed fit is symmetric, leading to the residual intensity that is present in the difference pattern for each peak. The peak tailing is present on the low d side of each reflection and is quite uniform. Since it is on the low d side, it is unlikely to be a result of axial divergence or other experimental set-up factors. This asymmetry is likely the result of planar defects, stacking and deformation faults, or turbostratic disorder, possibly introduced by the ball milling of the sample to obtain small particle size prior to being subjected to XRD. Programs such as MAUD, GSAS II, and FAULTS can account for such an asymmetry if the cause of the asymmetry is understood and appropriately modeled. In order to determine which of the potential sources of this asymmetry is present, a thorough microscopic study would need to be performed and a refinement with the appropriate disorder model could increase the occupancy detection differentiation.

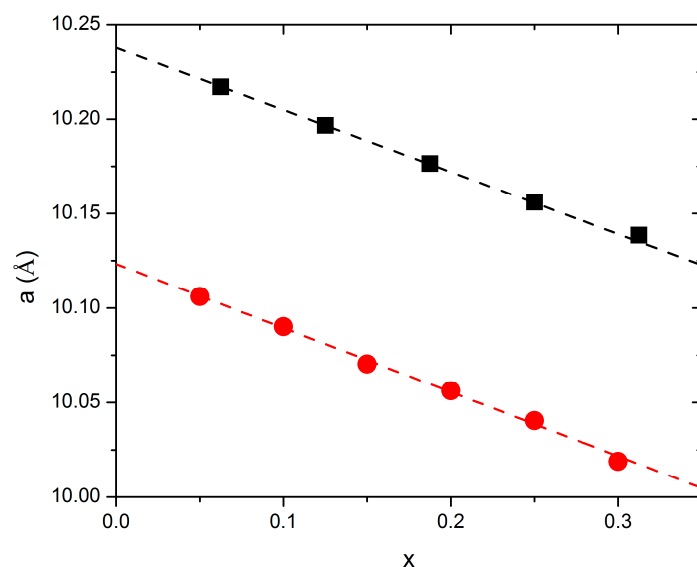


Figure S1. Experimental (circles) and computed (squares) lattice parameters (a) as a function of cosubstitution amount (x) for $\text{Mg}_x\text{In}_{2-2x}\text{Sn}_x\text{O}_3$ (circles) and $\text{Zn}_x\text{In}_{2-2x}\text{Sn}_x\text{O}_3$ (squares) with linear fits.

S1.3. $\text{Mg}_x\text{In}_{2-2x}\text{Sn}_x\text{O}_3$ Conductivity and Band Gap Measurements

As mentioned in the main article, the Seebeck coefficients of $\text{Mg}_x\text{In}_{2-2x}\text{Sn}_x\text{O}_3$ for each $x \leq 0.3$ are measured at 305 K and provided in Figure S4. These coefficients are negative and denote n-type character. The Seebeck coefficient is related to the conductivity and, as the conductivity universally increased after a reduction procedure, the Seebeck coefficients would be expected to increase (the absolute value would decrease), as in the case of $x = 0.30$. As can be observed from Figure S4, this is not the case and there is a wide variation between the Seebeck coefficients of a single composition. The reason for both of these phenomena is that the Seebeck measurement is sensitive to the size of the sample used. For these measurement, the sizes were not standardized, resulting in the variations in the values. Regardless as to these variations, however, all of the samples were negative, and the parity of the coefficient does not alter with size. Thus the n-type designation is sound, even though the data possess a high degree of variation.

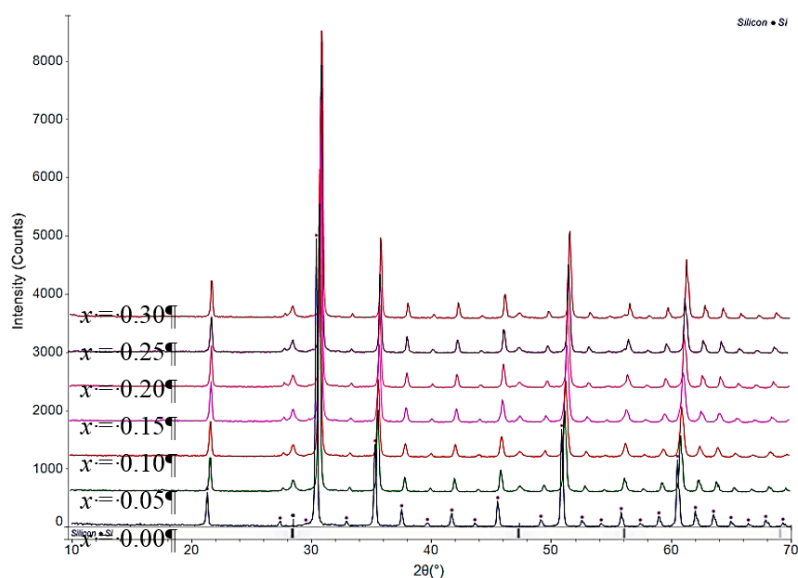


Figure S2. XRD patterns of $\text{Mg}_x\text{In}_{2-2x}\text{Sn}_x\text{O}_3$. Patterns are normalized to a Si standard that is displayed and all patterns exhibit the bixbyite structure, with no new peaks appearing. For comparison purposes, the pattern of In_2O_3 ($x = 0$) is shown without Si. The lattice contracts with increasing x .

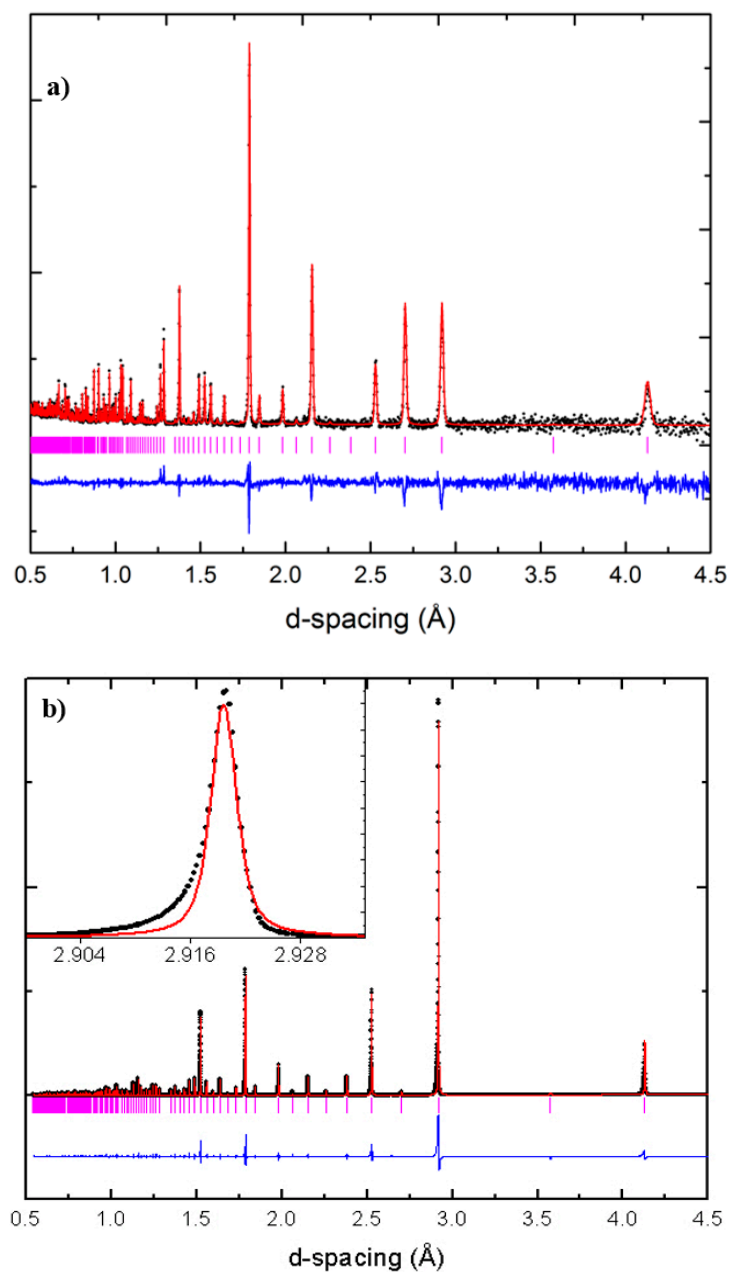


Figure S3. Sample (a) time-of-flight neutron and (b) synchrotron X-ray refinements of $\text{Mg}_{0.1}\text{In}_{1.8}\text{Sn}_{0.1}\text{O}_3$ with all of the Mg on the d-site. Every occupational model produces a similar fit, indistinguishable with a cursory inspection. Inset: close view of the major reflection, showing the asymmetry that is systematically present for all peaks. Black points are observed intensities, red lines are computed intensities, blue lines are the difference between calculated and computed, and the position of the Bragg reflections are denoted by vertical pink lines.

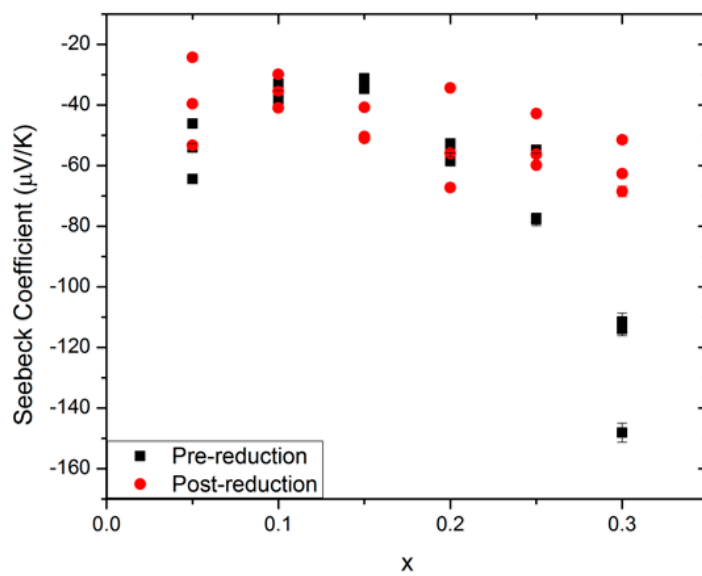


Figure S4. The Seebeck coefficients for 3 samples of $\text{Mg}_x\text{In}_{2-2x}\text{Sn}_x\text{O}_3$ at each value of x before (squares) and after (circles) being reduced. Error bars may be obscured by the data points.